Nonlinear Product Property Control in Industrial Gas-Phase Polyethylene Reactors

K. B. McAuley and J. F. MacGregor
Dept. of Chemical Engineering, McMaster University, Hamilton, Ontario, Canada L8S 4L7

A nonlinear model-based scheme is developed for product property control in industrial gas-phase polyethylene reactors. The controller regulates instantaneous melt index and density, and provides servocontrol during grade changeovers. Hydrogen and butene feed rates are manipulated to force the product properties onto desired trajectories. During grade changeovers, these trajectories are determined from off-line dynamic optimization studies. Optimal open-loop policies for reactor temperature, bleed stream flow, catalyst feed rate, and bed level are implemented as part of the changeover strategy.

The nonlinear feedback controller design is based on global input/output linearization methods. Disturbances are estimated, and plant/model mismatch is removed using an extended Kalman filter. Simulations on a complex mechanistic model of the process reveal that the nonlinear controller performs well for both regulatory and servocontrol. An analogous linear IMC controller is inadequate for disturbance rejection at different operating conditions and for control during grade changeovers. The simplicity of the nonlinear control algorithm makes it an interesting candidate for industrial application. This single controller can be used to control the properties of many grades of polyethylene made in the reactor and to accomplish near optimal changeovers between these grades.

Introduction

On-line control of polymer properties is difficult, because polymer reactors exhibit nonlinear dynamics, and the relationships between reactor operating conditions and product properties are complex (MacGregor et al., 1984). While traditional linear process models and controller design techniques have been successful for quality regulation about a single operating point, good servocontrol during grade transitions and regulation at different operating points often require mechanistic model-based control schemes to account for process nonlinearities. In this article, a nonlinear multivariable controller is developed for product property control in the industrial gas-phase polyethylene reactor shown in Figure 1. The performance of the proposed controller is compared with that of an analogous linear IMC design. Both product property regulation and grade transition control are addressed.

Correspondence concerning this article should be addressed to K. B. McAuley at the Department of Chemical Engineering, Queen's University, Kingston, Ontario, Canada K7L 3N6.

The feed streams to the polyethylene reactor comprise catalyst, inerts, ethylene, a butene comonomer, and hydrogen (Burdett, 1988; Choi and Ray, 1985). The feed gases act as fluidization and heat-transfer media, and supply reactants to the growing polymer particles. To maintain temperature control, the unreacted gases are cooled in an external exchanger before being recycled to the reactor. To prevent the accumulation of impurities and inerts, a small bleed stream is removed from the system. Periodically, polymer product is withdrawn from the reactor to keep the level of the fluidized bed near its setpoint. The main disturbances to product property control are reactive impurities in the feed stream and variations in catalyst properties.

For commercial linear polyethylenes, product properties are usually specified by melt index (MI) and density (ρ) (ASTM, 1990), which are related to the molecular weight and short-chain branching distributions of the polymer. The flexibility of gas-phase technologies, such as Union Carbide's UNIPOL

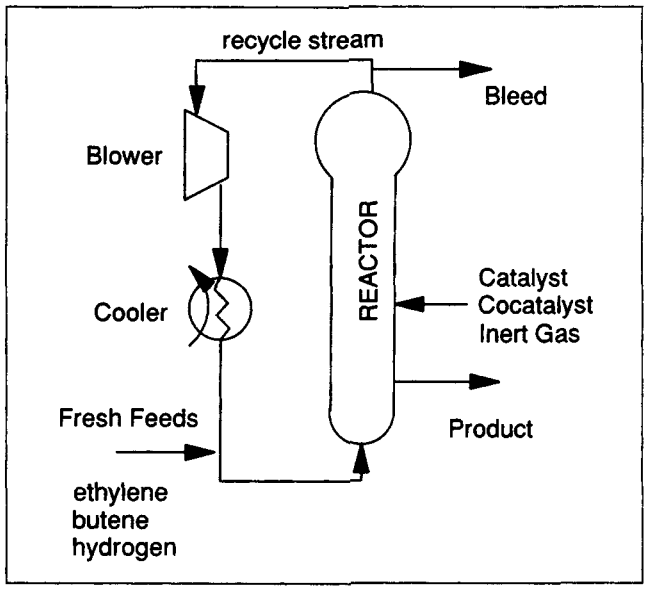

Figure 1. Industrial gas-phase polyethylene reactor.

process, allows production of a wide range of MI and ρ in a single reactor (Tait, 1989). Nevertheless, poorly executed transitions between successive polyethylene grades can result in large quantities of off-specification polymer being produced. Thus, optimization and control of grade transitions are of considerable economic importance.

One can assume that the MI and ρ of the polymer being produced in the reactor respond instantaneously to changes in gas composition and reactor temperature (McAuley and MacGregor, 1991). Hence, the dynamics associated with grade changeovers depend on the speed of changes in gas composition and temperature, and on the residence time of the polymer particles in the fluidized bed. When designing any product property controller, it is important to distinguish between the instantaneous polymer properties, MI_i and ρ_i, of the new polymer being formed, and the cumulative properties, MI_c and ρ_c, which are "averaged" properties for all of the polymer contained in the reactor.

Optimal-Grade Transition Trajectories

Before designing a control scheme for use during grade changeovers, it is important to know the best control performance achievable during product property transitions. For this reason, the authors performed a study of open-loop optimal changeover policies using dynamic model-based optimization techniques (McAuley and MacGregor, 1992). The manipulated variables considered in the study were the butene and hydrogen feed rates, the reactor temperature setpoint, the bleed stream flow, the catalyst feed rate, and the bed level setpoint. Although grade changeovers can be accomplished solely through manipulation of the hydrogen and butene feed rates, this type of policy can lead to long transition times and to the production of large quantities of off-specification polyethylene. Manipulation of the reactor temperature and the bleed stream flow rate can hasten grade transitions by increasing the rates of change of MI_i and ρ_i. Likewise, changes to the catalyst feed rate and the bed level can be used to influence both the polymer production rate and the solid-phase residence time.

Although transition policies suitable for on-line use have been determined, these open-loop optimal policies cannot be implemented directly. Implementation of nominal optimal manipulated variable policies, without accounting for disturbances or model mismatch, can lead to product property trajectories that differ significantly from the optimal property trajectories computed off-line. Feedback control during grade changeovers is required to ensure that large quantities of off-specification material are not produced.

On-Line Product Property Control

One method of performing feedback control during grade changeovers is to solve the full nonlinear dynamic optimization problem on-line at each control interval, using process measurements to provide information about disturbances and model mismatch. This methodology is conceptually simple and leads to the optimal transition policy, if the model is good and the disturbances are well-known (Bequette, 1991). It, however, requires excessive numerical computation and can be difficult to implement and maintain on-line. A simpler, albeit suboptimal, procedure is to use the open-loop optimal product property response as a reference trajectory to be followed by a nonlinear feedback controller. Using a nonlinear model-inverse-based design, an analytical expression can be developed for the manipulated variables. In this type of design, the computational load required by the controller is modest.

The following nonlinear feedforward/feedback control scheme has been designed and simulated. During grade transitions, the optimal open-loop policies for reactor temperature setpoint, bleed stream flow, catalyst feed rate, and bed level are implemented directly. To account for disturbances and model mismatch, the hydrogen and butene feed rates are used for feedback control. The objective of the feedback controller is to force MI_i and ρ_i onto their nominal trajectories determined in the off-line studies. For regulation about a steady state, the setpoint trajectory is constant and only the feedback portion of the controller is used. Choosing MI_i and ρ_i as controlled variables, rather than MI_c and ρ_c, is based on the philosophy that all new polymer produced in the remaining time should have properties as close as possible to target, regardless of the cumulative properties of the polymer already in the reactor.

Information flow in the control system

No on-line measurements are available for MI and ρ. Estimates of MI_i and ρ_i, which are required for feedback control, are inferred from the available on-line gas composition and temperature measurements, and from theoretically-based models (McAuley and MacGregor, 1991). Parameters in these models are updated every few hours using delayed off-line laboratory measurements of MI_c and ρ_c. The information flow in the control system is shown in Figure 2. Between laboratory measurements, the property inference scheme predicts $\hat{MI}_i$ and $\hat{\rho}_i$ using parameter estimates from the previous update step. The product property controller uses these property estimates, the setpoint trajectories, the model parameters, and the available on-line measurements to calculate control actions. The remainder of this article is concerned with the design and simulation of this model-based control algorithm.

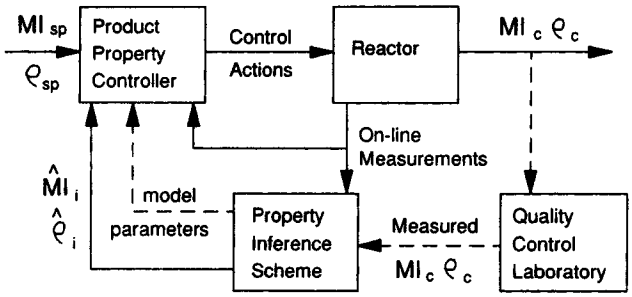

Figure 2. Product property controller information flow diagram.

Design of a Nonlinear Feedforward/Feedback Controller

Models for nonlinear controller design

The model used in the nonlinear controller design must be capable of predicting the effects of hydrogen and butene feed rates on instantaneous product properties. It should also account for changes in reactor temperature, bleed flow rate, catalyst feed rate, and bed level, because these variables change quickly during grade transitions. Additional disturbances, which should be addressed in the modeling procedure, include changes in reactive impurity levels and in catalyst properties. The proposed model consists of dynamic mass balances on hydrogen, butene, catalyst sites, and polymer, respectively:

$$\frac{d[H_2]}{dt} = \frac{1}{V_g}\left\{F_{H2} - k_H Y[H_2] - \frac{[H_2]b}{[C_T]} - g_i[H_2]\right\} \quad (1)$$

$$\frac{d[M_2]}{dt} = \frac{1}{V_g + V_s}\left\{F_{M2} - k_{p2} Y[M_2] - \frac{[M_2]b}{[C_T]} - S[M_2]O_p\right\} \quad (2)$$

$$\frac{dY}{dt} = F_{cat}a_{cat} - \frac{YO_p}{B_w} - k_d Y \quad (3)$$

$$\frac{dB_w}{dt} = Y\{k_{p1}[M_1]m_{w1} + k_{p2}[M_2]m_{w2}\} - O_p \quad (4)$$

$[H_2]$, $[M_1]$ and $[M_2]$ are the concentrations of hydrogen, ethylene and butene, respectively, in the gas phase. $[C_T]$ is the total concentration of all gas-phase components. V_g is the volume of gas in the reactor system, and V_s is the equivalent volume of butene dissolved in the polymer. F_{H2}, F_{M2} and F_{cat} are the respective fresh feed rates of hydrogen, butene and catalyst to the system. Y is the number of moles of active catalyst sites in the reactor, and a_{cat} is the active site concentration in the catalyst feed. B_w is the mass of polymer in the fluidized bed. k_H, k_{p1} and k_{p2} are kinetic rate constants for the consumption of hydrogen, ethylene and butene by the polymerization reactions. k_d is a catalyst site deactivation rate constant. b is the bleed stream flow rate, and O_p is the polymer outflow rate. g_i is a mismatch factor accounting for uncertainty in the hydrogen mass balance, and S is the solubility of butene in the polymer. m_{w1} and m_{w2} are the molecular weights of ethylene and butene, respectively.

Equations 1 to 4 can be integrated to predict the hydrogen and butene concentrations in the reactor, given the feed rates of hydrogen, butene and ethylene concentration, and the polymer outflow rate. In turn, MI_i and ρ_i can be calculated from the instantaneous property models developed by McAuley and MacGregor (1991). These models are of the form:

$$Y_1 = \ln(MI_i) = h_1([H_2], [M_1], [M_2], T) \quad (5)$$

$$Y_2 = \rho_i = h_2([H_2], [M_1], [M_2], T) \quad (6)$$

where T is the reactor temperature. The model structure in Eqs. 1 to 6 was chosen for use in the control design, because it is simple, yet it describes how the manipulated variables and reactor operating conditions influence the instantaneous product properties. To ensure that the model tracks the true behavior of the process, several model parameters must be updated on-line.

In this study, an extended Kalman filter (EKF) is used to update g_i, k_{p2}, k_d and O_p in Eqs. 1 to 4. This set of parameters was chosen, because the parameters affect the model states and, from our knowledge of the process, the value of each of these parameters can change due to reactor operating conditions. The four parameters can be estimated using on-line measurements of the gas-phase hydrogen and butene concentrations, the mass of polymer in the bed, and the instantaneous polymer production rate. Observability and consistency tests (Gagnon and MacGregor, 1991; Kozub and MacGregor, 1992b) reveal that all model and parameter states are observable from this set of measurements and that no sustained mismatch between measurements and model predictions occurs. Krishnan et al. (1992) present a more formal approach for choosing key model parameters for on-line updating and the best set of associated measurements. Using noisy measurements, the EKF is able to adjust the model parameters in response to temperature changes, production rate changes, and catalyst quality disturbances. Updates for parameters in Eqs. 5 and 6 are provided by the product property inference scheme.

The gas composition measurements from an on-line gas chromatograph are subject to measurement delay, h, of one GC sampling interval. As part of the EKF calculations, a one sampling interval forecast of the hydrogen and butene concentrations in the reactor is calculated. If these forecasts of the gas concentrations are used in Eqs. 5 and 6 instead of the measured values, then dead-time need not appear explicitly in the design of the control algorithm.

Nonlinear controller design

An important concept in nonlinear controller design is the relative order of the process model. Relative order can be explained intuitively as the inherent integration between the process input and output. If the hydrogen and butene feed rates are used to control MI_i and ρ_i, then the relative order of the system is one, because the hydrogen and butene feed rates are each integrated once to obtain either MI_i or ρ_i. Many nonlinear control algorithms are suitable for relative-order-one systems. Use of the reactor temperature setpoint as a manipulated variable for melt index control leads to a system with a relative order greater than one, and to a more complex nonlinear control algorithm.

A second important concept for designing and analyzing nonlinear control laws is that of the tracking error trajectory

(McLellan et al., 1990). The closed-loop error trajectory for any process can be defined as:

$$\underline{e}(t) = \underline{Y}_{sp}(t) - \underline{Y}(t) \tag{7}$$

where $\underline{Y}$ and $\underline{Y}_{sp}$ are vectors of output variable trajectories and setpoint trajectories, respectively. Many control laws can be derived by specifying the type of closed-loop error trajectory that the system will follow in response to a deviation from setpoint. The simplest error trajectory specification used in the design of nonlinear model-based controllers (Freund, 1982; Kozub and MacGregor, 1992a) is the following decoupled first-order specification:

$$\dot{\underline{e}}(t) = \underline{K}\underline{e}(t) \tag{8}$$

where $\underline{K}$ is diagonal. Controller tuning is accomplished by changing the elements of $\underline{K}$ which are the negative reciprocals of the desired first-order closed-loop time constants of the response. A second commonly used error trajectory specification is a decoupled second-order response which is used in the generic model control (GMC) designs of Lee and Sullivan (1988). Controllers designed with either first- or second-order linear error trajectory descriptions are a special case of the global linearizing control (GLC) algorithm of Kravaris and Chung (1987). Whereas the first-order trajectory in Eq. 8 leads to an exponential decay of the error and cannot be used to accommodate overshoot in the closed-loop response, a second-order specification is capable of producing either an overdamped or underdamped second-order error response, depending on the choice of tuning constants. An additional benefit of the second-order specification is that controllers designed using this criterion automatically contain integral action (McLellan et al., 1990). Integral action is required to eliminate steady-state offset between the setpoint trajectory and controlled variables, arising due to sustained mismatch between model predictions and measured outputs. However, explicit incorporation of integral action in the current product property control algorithm is unnecessary, because the EKF and product property inference scheme contain the integral action necessary to eliminate steady-state offset between model predictions and product properties. This integral action in the state and property estimators results from the use of nonstationary models for stochastic and parameter states in these estimators, and does not rely on the process and property models being perfect. In the simulation results reported in this article, there is structural mismatch between the full plant model (McAuley, 1992) used to test the controller and the reduced model in Eqs. 1 to 4. Gagnon and MacGregor (1991) and Kozub and MacGregor (1992b) discuss the use of nonstationary parameter states in state estimation problems.

The simpler first-order specification has been chosen for the controller design, because integral action is not required in the controller itself, and an exponential decay in the error response is desirable in this application. The first-order error trajectory specification in Eq. 8 can be expressed as:

$$\dot{Y}_1 = \dot{Y}_{1sp} - \kappa_1 (Y_{1sp} - Y_1) \tag{9}$$

$$\dot{Y}_2 = \dot{Y}_{2sp} - \kappa_2 (Y_{2sp} - Y_2) \tag{10}$$

where κ_1 and κ_2 are the diagonal elements of $\underline{K}$. During a grade changeover, the values of Y_{1sp}, Y_{2sp} and their time derivatives are obtained from the open-loop optimal product property trajectories. During regulation at a target grade, Y_{1sp} and Y_{2sp} are constants, and $\dot{Y}_{1sp}$ and $\dot{Y}_{2sp}$ are both zero. Assuming a constant ethylene concentration in the reactor and differentiating Eqs. 5 and 6 with respect to time give:

$$\dot{Y}_1 = \frac{\partial h_1}{\partial [H_2]}\frac{d[H_2]}{dt} + \frac{\partial h_1}{\partial [M_1]}\frac{d[M_1]}{dt} + \frac{\partial h_1}{\partial [M_2]}\frac{d[M_2]}{dt} + \frac{\partial h_1}{\partial T}\dot{T} \tag{11}$$

$$\dot{Y}_2 = \frac{\partial h_2}{\partial [H_2]}\frac{d[H_2]}{dt} + \frac{\partial h_2}{\partial [M_1]}\frac{d[M_1]}{dt} + \frac{\partial h_2}{\partial [M_2]}\frac{d[M_2]}{dt} + \frac{\partial h_2}{\partial T}\dot{T} \tag{12}$$

Since the ethylene concentration in the reactor is regulated by an ethylene partial pressure controller, $d[M_1]/dt$ in Eqs. 11 and 12 is small and can be neglected. The partial derivatives of h_1 and h_2 with respect to hydrogen concentration, butene concentration, and temperature can be obtained analytically from Eqs. 5 and 6 (McAuley, 1992). Eliminating $\dot{Y}_1$ and $\dot{Y}_2$ from Eqs. 9 to 12 and solving for $d[H_2]/dt$ and $d[M_2]/dt$ yield the following expressions:

$$\frac{d[H_2]}{dt} = \frac{\dfrac{\partial h_2}{\partial [M_2]}M - \dfrac{\partial h_1}{\partial [M_2]}N}{\dfrac{\partial h_2}{\partial [M_2]}\dfrac{\partial h_1}{\partial [H_2]} - \dfrac{\partial h_1}{\partial [M_2]}\dfrac{\partial h_2}{\partial [H_2]}} = P \tag{13}$$

$$\frac{d[M_2]}{dt} = \frac{M - \dfrac{\partial h_1}{\partial [H_2]}P}{\dfrac{\partial h_1}{\partial [M_2]}} = Q \tag{14}$$

where

$$M = \dot{Y}_1 - \kappa_1 (Y_{1sp} - Y_1) - \frac{\partial h_1}{\partial T}\dot{T} \tag{15}$$

$$N = \dot{Y}_2 - \kappa_2 (Y_{2sp} - Y_2) - \frac{\partial h_2}{\partial T}\dot{T} \tag{16}$$

Eliminating $d[H_2]/dt$ and $d[M_2]/dt$ from Eqs. 1, 2, 13 and 14 gives the following expressions for the manipulated variables F_{H2} and F_{M2} in terms of known quantities:

$$F_{H2} = (P + L) V_g \tag{17}$$

$$F_{M2} = (Q + W)(V_g + V_s) \tag{18}$$

$$L = \frac{k_H Y[H_2] + \dfrac{[H_2]b}{C_T} + g_l[H_2]}{V_g} \tag{19}$$

$$W = \frac{k_{p2} Y[M_2] + \dfrac{[M_2]b}{C_T} + S[M_2]O_p}{V_g + V_s} \tag{20}$$

Equations 17 and 18 are algebraic expressions for the hydrogen and butene feed flow rates required to achieve the performance specification in Eqs. 9 and 10. Thus, the nonlinear control law itself is very simple and can be implemented in a few lines of computer code. The majority of the effort required to implement and maintain this type of controller will be associated with integrating the model in Eqs. 1 to 4, and with coding and testing the EKF. Similar model integration and updating steps would be required if a nonlinear programming approach were adopted to solve this problem. Since estimates of the current gas compositions are available from the EKF every $h=0.1417$ time periods, a discrete version of the nonlinear controller with sampling interval h has been implemented and tested on the full nonlinear plant model.

Linear Analog to the Nonlinear Feedforward/Feedback Controller

To illustate the effectiveness of the combined EKF and nonlinear control law, its performance must be compared with that of a known standard controller. Fortunately, it can be shown that a linear decoupled internal model control (IMC) design provides a linear analog to the nonlinear control design described above. The derivation of this linear IMC controller is presented in the Appendix, and the structure is shown in Figure 3, wherein $\underline{G}^*$ and $\underline{D}^*$ represent the true process. This is a standard IMC feedback control structure, with added feedforward action. $\underline{Y}_{sp}(t+2h)$, the two-step-ahead prediction of the product property setpoints, is required in the control formulation. It is constant for regulation at a single grade, and during grade changeovers, the future setpoints can be obtained from optimal-grade transition trajectories determined by McAuley and MacGregor (1992). Note that the setpoint trajectory is not filtered, but first-order filtering is performed along the disturbance and mismatch path. The identification of linear transfer function models for this IMC controller is discussed below.

Transfer model identification for the linear controller

A series of step tests was performed on the full nonlinear plant model to determine the set of discrete transfer function models shown in Table 1. The sampling interval for these models is $h=0.1417$ time periods, which is equal to the GC sampling interval. The linear feedforward/feedback controller was tested on optimal changeover policies that use only the bleed flow and reactor temperature as feedforward variables. As a result, transfer function models for catalyst feed and bed level changes were not obtained. The transfer functions in Table 1 were identified from the response of the full theoretically-based model to a series of small upward and downward steps about the operating conditions for Grade A. Note that all scaling used in this article is consistent with previous articles (McAuley et al., 1990; McAuley and MacGregor, 1991, 1992; McAuley, 1992).

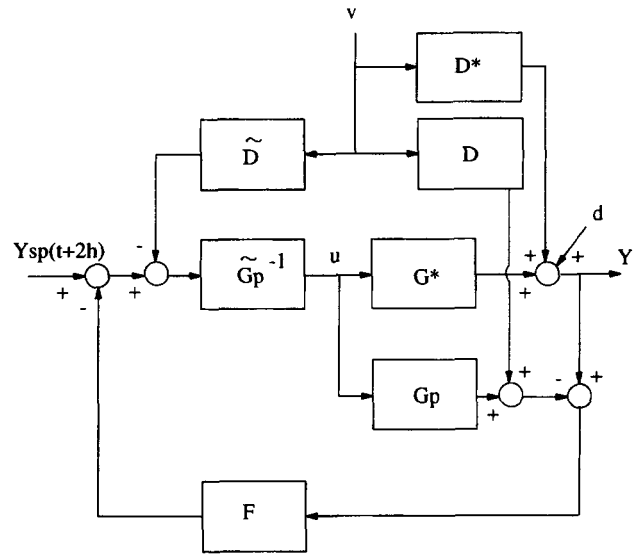

Figure 3. Linear IMC analog of the nonlinear feedforward/feedback controller.

Nominal performance of the linear IMC controller

An IMC controller was designed using the models in Table 1 and the structure in Figure 3. Both m_1 and m_2 were set at 0.8679 to correspond to desired first-order closed-loop time constants of one time period. To test the performance of this controller in the absence of the plant/model mismatch, linear transfer function models from Table 1 were used in $\underline{G}^*$. The

Table 1. Transfer Function Models Used in IMC Design

	Scaled Output Deviation Variable	
Scaled Input Dev. Variable	Y_1 $\ln(MI_i)$	Y_2 ρ_i
u_1 Hydrogen Feed	$\dfrac{0.1605z^{-2}}{1-0.9856z^{-1}}$	$\dfrac{0.1644z^{-2}}{1-0.9835z^{-1}}$
u_2 Butene Feed	$\dfrac{0.1576z^{-2}}{1-0.8891z^{-1}}$	$\dfrac{-1.5776z^{-2}}{1-0.9023z^{-1}}$
v_1 Temp. Setpoint	$\dfrac{0.7596z^{-2}-0.8298z^{-3}-0.05152z^{-4}+0.1306z^{-5}}{1-0.9748z^{-1}}$	$\dfrac{-0.004473z^{-2}+0.03579z^{-3}}{1-0.7091z^{-1}}$
v_2 Bleed Valve Position	$\dfrac{-0.02269z^{-2}}{1-0.9771z^{-1}}$	$\dfrac{0.001054z^{-2}-0.001065z^{-3}}{1-1.728z^{-1}+0.7324z^{-2}}$

nominal response of this linear control system was tested, with and without measurement noise, for setpoint changes, disturbance rejection, and changes in the feedforward variables, assuming that MI_i and ρ_i measurements were available every $h=0.1417$ time periods (McAuley, 1992). As specified in the design, for noise-free measurements, the closed-loop output response of the system is perfectly decoupled, setpoint trajectories are followed exactly, and the controller is able to compensate perfectly for changes in the reactor temperature setpoint and the bleed flow rate.

Performance of the Nonlinear and Linear Control Schemes of the Full Nonlinear Plant Model

In this section, the performance of the control system is evaluated for both disturbance rejection and setpoint tracking, assuming that the values of MI_i and ρ_i are available every $h=0.1417$ time periods, where h is the GC sampling interval. In practice, these values are not measured on-line, but can be estimated from the GC measurements using instantaneous property models (Eqs. 5 and 6) and the inferential methods of McAuley and MacGregor (1991). The results of this combined inference and nonlinear control scheme are discussed in a separate section. The tuning parameters for the nonlinear controller, κ_1 and κ_2, have both been set at -1, resulting in a closed-loop time constant of one time period. This is the same performance specification used in the linear controller design.

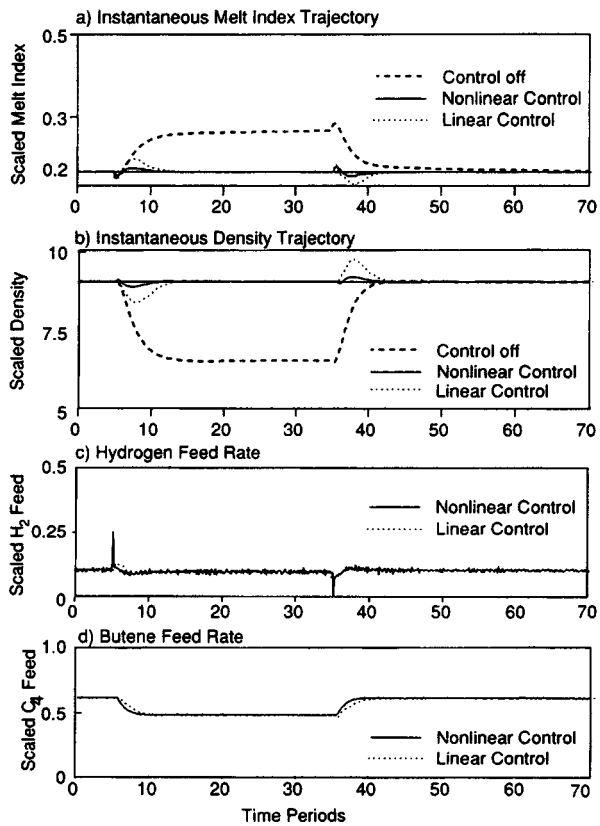

Figure 4. Responses of linear and nonlinear controllers to catalyst disturbances.

Disturbance rejection

Catalyst variability is an important source of disturbances in the control of gas-phase polyethylene reactors. Figure 4 shows the response of MI_i and ρ_i to a 30% reduction in the active site concentration on the catalyst. This change occurs at time 5 and continues until time 35 when feeding of the original catalyst resumes. Without product property control, this disturbance causes a significant change in both MI_i and ρ_i. Fewer active catalyst sites in the reactor cause the production rate and hence the butene consumption rate to fall. As the butene concentration increases, MI_i increases and ρ_i falls. As shown in Figure 4, either the nonlinear controller and EKF or the linear IMC controller can be used to alleviate the effects of the catalyst disturbance. Both controllers act by reducing the butene feed rate, thereby bringing the butene concentration in the reactor back to the required level.

When the nonlinear controller is used, the EKF detects a change in the polymer production rate induced by the catalyst disturbance. The EKF compensates by changing k_d, which affects Y, the estimated number of catalyst sites in the reactor. Because the EKF updates these parameters, there is no steady-state offset between the product properties and their setpoints, even though the controller itself does not contain integral action, and the structure of the model used in the controller is different from that used in the plant simulation. Using the updated value of k_d, the EKF is able to predict a reduction in butene consumption, and the controller takes immediate action to reduce the butene feed rate accordingly.

The linear controller must wait until an actual increase in the butene concentration is observed, and a change in both MI_i and ρ_i is predicted, before appropriate feedback action can be taken. The linear controller is not as effective as the nonlinear controller in defending against catalyst disturbances, mainly because the linear transfer function models do not contain any information about how catalyst disturbances affect MI_i or ρ_i. In Figure 4, the performance improvement associated with using the nonlinear control system, not the linear controller, is due mainly to the EKF, rather than any nonlinearities in the system.

The disturbance rejection tests in Figure 4 were conducted at the same conditions where the linear transfer function models in the IMC controller were identified (at Grade A). The same catalyst disturbance was simulated while producing Grade C ($MI_i=2.4$, $\rho_i=13$). While the nonlinear controller rejected the catalyst disturbance equally well at both grades, the linear controller's performance degraded significantly. With the linear controller, both MI_i and ρ_i required approximately twice as long to return to their setpoints as was required in Figure 4. The MI and ρ setpoints corresponding to Grades A, B and C in Table 2 are the same values as those in McAuley and MacGregor (1992). Gain scheduling or use of a separate linear controller for each grade could have been used to obtain satisfactory

Table 2. Melt Index and Density Setpoints for Three Polyethylene Grades

	Scaled Melt Index	Scaled Density
Grade A	0.2	9
Grade B	0.16	13
Grade C	2.4	13

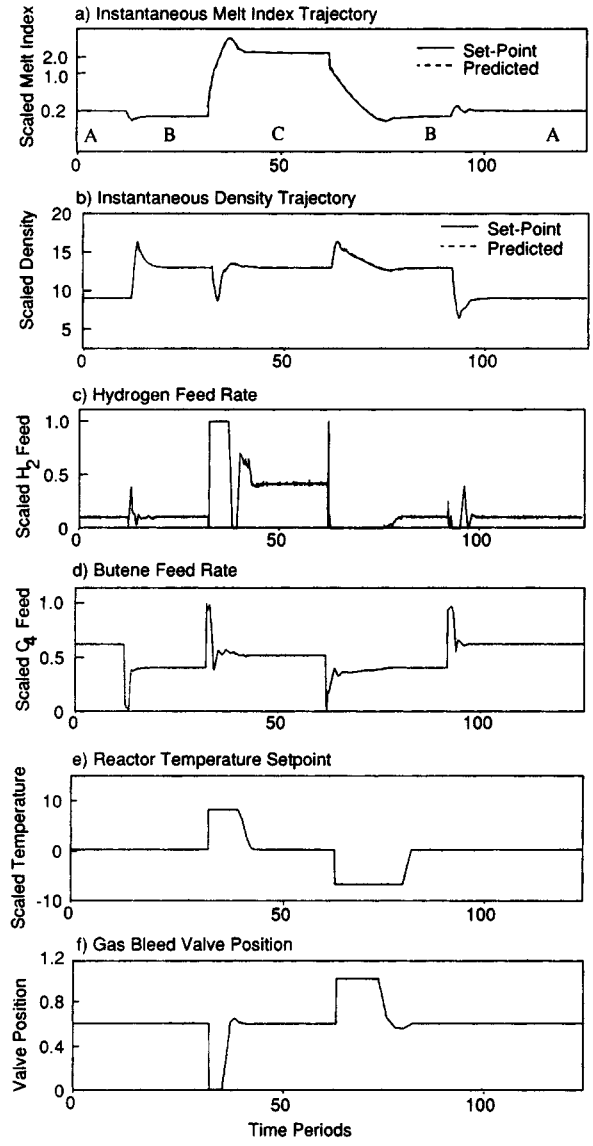

Figure 5. Performance of nonlinear feedforward/feedback controller during grade changeovers.

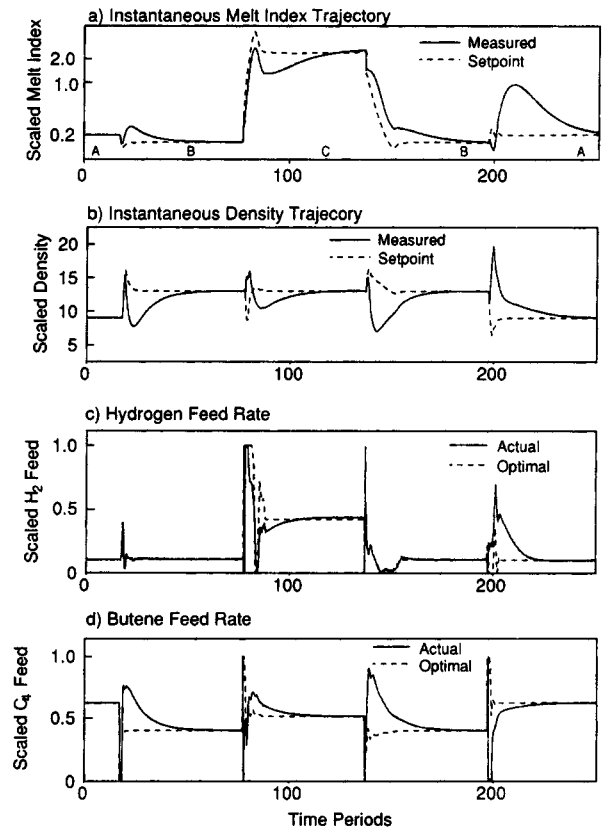

Figure 6. Performance of linear IMC controller during grade changeovers.

disturbance rejection during the production of a number of different polyethylene products. However, judging from the results shown in the next section, it is unlikely that such an approach would be successful when changing from one product grade to the next. The main benefit of using a nonlinear controller design is that a single controller can be used successfully for all grades and for grade changeovers.

Control during grade changeovers

In Figure 5, the nonlinear controller is used to follow a series of grade changeovers ($A \rightarrow B$ at $t=12$, $B \rightarrow C$ at $t=32$, $C \rightarrow B$ at $t=62$, and $B \rightarrow A$ at $t=92$). In the changeover policy used for the $A \rightarrow B$ and $B \rightarrow A$ transitions, hydrogen and butene are used as manipulated variables. As a result, only the feedback portion of the nonlinear controller is used during these transitions. During the $B \rightarrow C$ and $C \rightarrow B$ transitions, the reactor temperature setpoint and bleed valve position are included as feedforward variables. In these two transitions, both the feedforward and feedback capabilities of the nonlinear controller are tested. As shown in Figure 5, the nonlinear controller follows the desired instantaneous product property trajectories very closely. Slight deviations between the desired and actual trajectories are due to short-term mismatch induced by the large temperature changes affecting the parameters updated by the EKF. The nonlinear controller also performs well when all four feedforward variables (temperature, bleed, bed level, and catalyst feed) are used to accomplish grade changeovers (McAuley, 1992).

The ability of the linear controller to accomplish the same set of grade transitions is shown in Figure 6. It is readily apparent that the linear controller's performance is inadequate for implementing optimal-grade changeover policies. Note that the time scale in Figure 6 is different from that in Figure 5 and that successive grade transitions are performed further apart in time. The expanded time scale is required, because the linear controller takes a long time to bring the product properties to their steady-state positions. The reason for the poor controller performance during the $A \rightarrow B$ and $B \rightarrow A$ transitions is the poor predictive ability of the transfer function models used to design the feedback portion of the IMC controller. Since the responses of $\ln(MI_i)$ and ρ_i to changes in the hydrogen and butene feed rates are very nonlinear, the linear models used in the controller design are not able to provide adequate predictions of product property behavior. When the reactor is operated away from Grade A, where the transfer function models were identified, changes in both the time constant and the gain of product property responses are large.

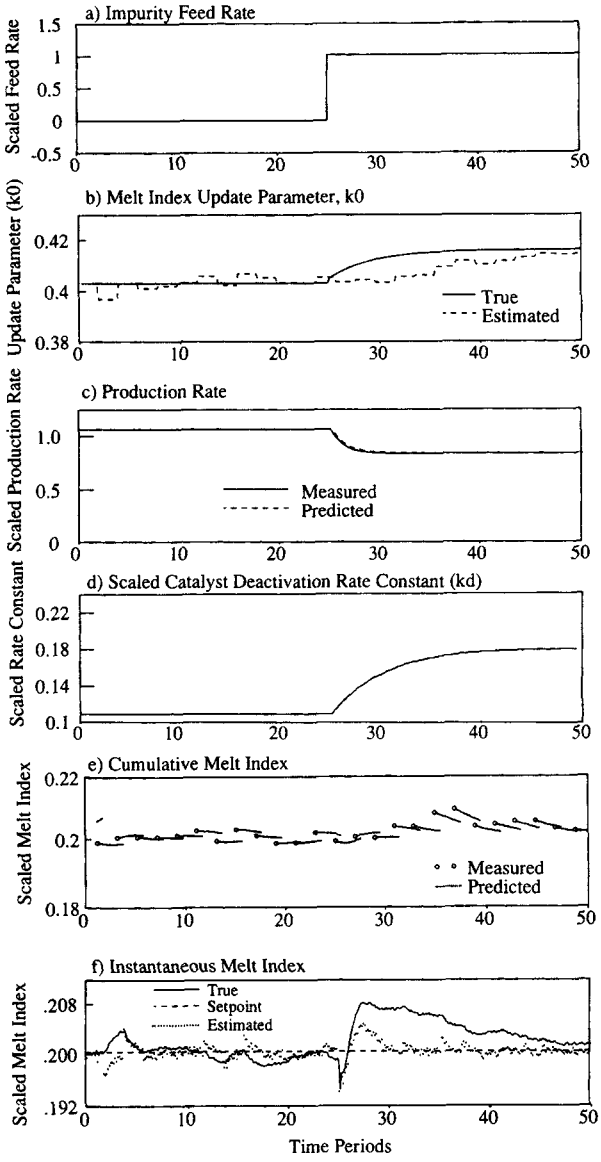

Figure 7. Response of combined property inference scheme and nonlinear controller to an impurity disturbance.

The resulting plant/model mismatch is interpreted by the controller, as if it were caused by an output disturbance. During the $B \rightarrow C$ and $C \rightarrow B$ transitions, the poor performance of the linear controller is due to inadequate predictions by both the feedforward and feedback transfer function models. Although the linear controller is unable to follow the optimal trajectories, it is able to bring the product properties to their desired steady-state values, given a sufficient amount of time.

Combining the Product Property Inference Scheme with the EKF and Nonlinear Controller

Since on-line measurements of the product properties are not available, estimates of the current values of MI_i and ρ_i are supplied by an on-line product property inference scheme (McAuley and MacGregor, 1991). Information flow between this inference scheme and the product property controller is

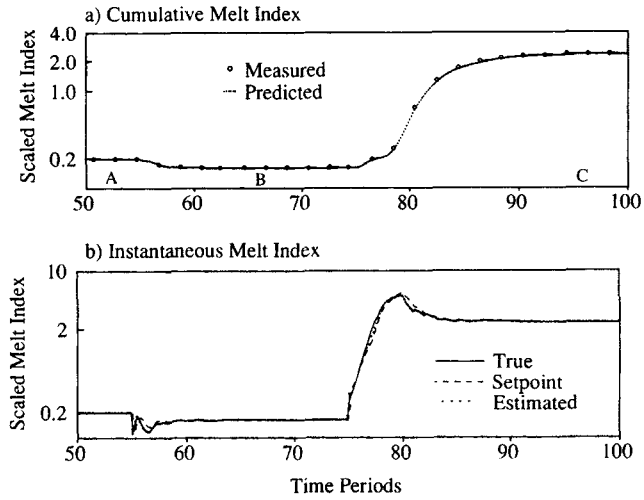

Figure 8. Performance of combined property inference scheme and nonlinear controller during grade changeovers after the catalyst disturbance.

shown in Figure 2. In this diagram, both the nonlinear controller and the EKF are contained in the box labeled product property controller. Simultaneous operation of the nonlinear controller, the EKF, and the product property controller was demonstrated using simulated laboratory data, with the same measurement noise levels experienced in the actual process.

As shown in Figure 7, the control scheme is able to reject a disturbance resulting from reactive impurities in the feed stream. Beginning at time period 35, as the impurity level in the reactor increases, active catalyst sites are killed, resulting in a drop in production rate. In addition, growing polymer chains are terminated, resulting in a decrease in molecular weight and a corresponding increase in melt index. The EKF accounts for the observed change in production rate by increasing k_d, the catalyst deactivation rate parameter, shown in Figure 7d. As a result, the controller reduces the butene feed rate to prevent the density from deviating from setpoint.

Rising impurity levels cause the true value of k_0, the impurity-sensitive adjustable parameter in Eq. 5 to increase. Between time periods 35 and 45, the on-line inference scheme consistently underestimates MI_c by a small amount. To remove this offset, the parameter updating portion of the inference scheme adjusts the estimate of k_0 toward its true value as shown in Figure 7b. The nonlinear controller is able to control the estimated value of MI_i as its setpoint after only a few hours. Nevertheless, the true value of MI_i remains above its target until feedback from the laboratory measurements can be used to update k_0 in the instantaneous melt index model. This updating takes a considerable amount of time, because the differences between the estimated and measured values of MI_c are very small. Larger deviations would result in faster updating (McAuley and MacGregor, 1991).

With the same impurity level in the feed, a set of grade changeovers was simulated, and the MI response is shown in Figure 8. Although impurities were not considered in the off-line optimization of the setpoint trajectory in Figure 8b, good performance was achieved during the changeovers. In conclusion, the combined nonlinear controller, EKF and on-line inference scheme perform well for both rejection of impurity

disturbances and for grade changeovers affected by a change in impurity levels.

Manipulated Variable Saturation

During optimal grade changeovers, the hydrogen and butene feed rates are held at their bounds for extended periods of time. Therefore, the feedback controller used for grade changeovers must be able to deal adequately with manipulated variable saturation. The simulations in Figures 5 to 8 have not used optimal saturation handling procedures; however, because implemented values, rather than calculated control actions, were used in all subsequent calculations, wind-up was prevented. In this section, an optimal means of handling manipulated variable saturation for the nonlinear feedforward/feedback controller is assessed, and a variable structure controller design that provides an additional degree of freedom when the hydrogen feed rate saturates is proposed.

The input saturation problem is easily handled for linear multivariable controllers (Segal et al., 1991), and a similar approach can be adopted for multivariable nonlinear controllers. The problem of identifying saturated input variables and setting them to their limiting values is analogous to the linear control problem. In the nonlinear control problem, however, no general closed-form solution is available to determine the optimal position of the remaining unbounded variables. Spong et al. (1986) suggest determining the positions of the unconstrained manipulated variables by solving a quadratic program on-line. However, for the 2×2 system considered in this article, when one manipulated variable saturates, only one free variable must be determined, and an analytical solution can be found. Without manipulated variable saturation, the control performance specification is given by Eqs. 9 and 10. When one manipulated variable saturates, both of these equations cannot be solved simultaneously. The best that can be achieved is to minimize the weighted sum of squares:

$$J = w\{\dot{Y}_{1sp} - \dot{Y}_1 - \kappa_1(Y_{1sp} - Y_1)\}^2 + \{\dot{Y}_{2sp} - \dot{Y}_2 - \kappa_2(Y_{2sp} - Y_2)\}^2 \quad (21)$$

where w weights the relative importance of satisfying Eqs. 9 and 10. If u_1 saturates, one must determine u_2 so that:

$$\frac{\partial J}{\partial u_2} = 0 \quad (22)$$

This condition is satisfied at only one value of u_2, which can be determined by substituting Eqs. 1, 2 and 9 to 12 into Eq. 21 and differentiating with respect to u_2. A similar expression can be derived for u_1 when u_2 saturates.

Using this approach, McAuley (1992) has tested the system response to hydrogen feed saturation during a $B\rightarrow C$ transition with the hydrogen feed rate limited at 90% of its normal maximum value, for several values of w. As expected, large values of w resulted in only small deviations in melt index (Y_1). Conversely, a very small value of w can be used to obtain good density control (Y_2), at the expense of large deviations in MI. With a moderate value of w, the output response of the system was nearly identical to that obtained without optimal saturation handling, using actually implemented past flow rates in the algorithm.

So far, the discussion of manipulated variable saturation has assumed a square controller structure, with hydrogen and butene feed rates as the manipulated variables. If the performance of this controller proves unsatisfactory and the manipulated variables are often at their bounds, then an additional manipulated variable could be incorporated into the feedback control scheme. For example, if saturation of the hydrogen feed is a common problem, perhaps the best choice for an additional manipulated variable is the bleed stream flow rate. Opening or closing the bleed valve when the hydrogen saturates could be used to hasten the return of MI_i and ρ_i onto their desired trajectories. Although a full nonlinear programming approach could automatically handle this nonsquare control problem, the approach described here requires less on-line computation.

Since the relative order between b and both MI_i and ρ_i is unity, the design of this 3×2 variable structure nonlinear controller is straightforward. Equations 17 and 18 can be rearranged to give two algebraic equations of the form:

$$f_1(F_{H2}, F_{M2}, b) = 0 \quad (23)$$

$$f_2(F_{H2}, F_{M2}, b) = 0 \quad (24)$$

which must be satisfied to ensure that MI_i and ρ_i follow the desired trajectories specified in Eqs. 9 and 10. When neither the hydrogen nor the butene feed rate is saturated, this condition can be satisfied by implementing F_{H2} and F_{M2} from Eqs. 17 and 18, with the bleed flow rate at its desired setting, b_{des}. When the hydrogen feed is saturated, Eqs. 23 and 24 can still be satisfied by setting F_{H2} at its limiting value and solving for appropriate values of F_{M2} and b. Once the value of F_{H2}, calculated using b_{des} in Eq. 17, is no longer saturated, the bleed flow rate can be returned to its desired value, and use of the original control calculations in Eqs. 17 and 18 can be resumed.

Statistical Process Control

Once an advanced control system has been implemented to control polymer properties, further quality improvements can be realized by superimposing a statistical process monitoring scheme on top of the feedforward/feedback control system. The objectives of both the feedforward/feedback control scheme and the statistical process monitoring/control (SPC) scheme are the same: both improve control over product quality. They, however, achieve these objectives in fundamentally different, but very complementary, ways. The feedforward/feedback process control system reduces the effect of process variability arising from disturbances by transferring the predictable component of the variability from the final product properties into the manipulated variables (see, for example, Downs and Doss, 1991). Statistical process control schemes attempt to reduce variability in the process using tools such as control charts (Shewart, T^2, and so on) (John, 1991) to monitor the important product properties and to detect special events that differ from normal common causes of process variation. The approach is to search for assignable causes for these special events and then to remove as many of those causes as possible from the process, thereby eliminating variability and improving the process over the long term.

A criticism often leveled at the use of only feedforward/

feedback process control in quality control situations is that the control systems compensate for both common cause and special cause variation alike, and often mask the presence of disturbances arising from special events, such as the large catalyst activity change occurring between periods 5 and 35 in Figure 4. However, this need not be the case, if an SPC scheme is superimposed on top of the control system. The variability in the process has not been eliminated by the feedforward/feedback control scheme, just transferred to the other variables. Therefore, by applying SPC methods to the manipulated variables (hydrogen and butene feeds) in Figure 4, the occurrence of a special event is easily detected at periods 5 and 35. Alternatively, in any model-based control scheme, such as the IMC scheme in Figure 3, an estimate of the disturbance, $\underline{d}$, which would have occurred if no control action had been taken is always available and can be plotted on control charts.

It can also be argued that model-based process control schemes can greatly enhance the ability to perform SPC by providing more information on the possible sources of the disturbances. For example, in the nonlinear control scheme developed in this article, an EKF and product property inference scheme are continually providing estimates of important disturbance states such as the catalyst deactivation rate constant (k_d), the butene consumption rate parameter (k_{p2}), hydrogen mass balance errors (g_l), and impurity levels (k_0). By plotting these disturbance state estimates on control charts, one might much more easily detect special events and diagnose the special causes behind them. In summary, it is important that one obtain the best results from applying both feedforward/feedback process control and statistical process control in any quality control application.

Conclusions

A nonlinear model-inverse-based feedback controller has been designed for product property control in industrial gas-phase polyethylene reactors. This feedback controller manipulates hydrogen and butene feed rates to defend against disturbances and to follow optimal trajectories for instantaneous MI and ρ. Open-loop optimal policies for the reactor temperature setpoint, bleed stream flow rate, catalyst feed rate, and bed level are implemented as part of the grade changeover strategy. An EKF is used to estimate unmeasured disturbances and to remove any plant/model mismatch by updating model states and parameters. Although this approach to product property control can lead to suboptimal transitions when disturbances occur, the computational simplicity makes it a much better candidate for on-line implementation than an optimal controller based on nonlinear programming techniques.

The performance of the nonlinear controller is far superior to that of a linear controller with the same performance specification, indicating that proper accounting for nonlinearities is essential to good product property control in gas-phase polyethylene reactors. The simultaneous operation of the nonlinear controller, EKF and product property updating scheme was tested for both an impurity disturbance and grade changeovers.

This nonlinear control system would appear to offer great potential for implementation on industrial fluidized-bed polyethylene processes, as well as on other continuous chain growth polymerization processes that produce a variety of polymer grades. It provides a single powerful controller capable of controlling polymer properties for the many product grades produced at different reactor conditions, and it is capable of accomplishing near-optimal changeovers between grades. This model-based controller is also suitable for implementation as part of an overall product quality control scheme involving both feedforward/feedback control and statistical process control.

Acknowledgment

The authors would like to acknowledge financial support from the National Science and Engineering Research Council of Canada.

Notation

a_{cat} = number of catalyst sites per unit mass of catalyst
b = bleed stream flow rate
B_w = mass of polymer in the reactor
$[C_T]$ = combined concentration of gas phase components
$\underline{d}$ = disturbance faced by linear controller
$\underline{D}$ = linear feedforward transfer function model
$\underline{\tilde{D}}$ = linear feedforward transfer function model with dead time removed
$e(t)$ = error trajectory
f_1, f_2 = functions in Eqs. 33 and 34, which must be zero to achieve specified control performance
$\underline{F}$ = IMC feedback filter
F_{H2}, F_{M2}, F_{cat} = feed rates of hydrogen, butene and catalyst
g_l = hydrogen gas loss parameter
$\underline{G_p}$ = linear process transfer function model
$\underline{\tilde{G}_p}$ = linear process transfer function model with dead time removed
h = gas sampling and controller discretization interval (0.1417 time periods in the applications)
h_1, h_2 = output equations for $\ln(MI_i)$ and ρ_i
$[H_2]$ = hydrogen concentration in the gas phase
$\underline{I}$ = identity matrix
J = performance index for optimal saturation handling
κ_1, κ_2 = nonlinear controller tuning factors
k_d = catalyst deactivation rate constant
k_H = rate constant for hydrogen consumption
k_{p1}, k_{p2} = rate constants for ethylene and butene consumption
$\underline{K}$ = diagonal matrix for tuning nonlinear controller
L = parameter defined in Eq. 19
M = expression defined in Eq. 15
$\underline{M}$ = diagonal matrix for linear controller tuning
m_1, m_2 = diagonal elements of $\underline{M}$ matrix
$[M_1], [M_2]$ = ethylene and butene concentrations in the gas phase
MI_c, ρ_c = cumulative melt index and density
MI_i, ρ_i = instantaneous melt index and density
MI_{sp}, ρ_{sp} = setpoints for instantaneous melt index and density
N = expression defined in Eq. 16
O_p = polymer outflow rate
P = expression defined in Eq. 13
Q = expression defined in Eq. 14
S = butene solubility coefficient
t = time
T = reactor temperature
τ = first-order closed-loop time constant
$\underline{u}$ = vector of manipulated variables
$\underline{v}$ = vector of feedforward variables
V_g = volume of the gas phase
V_s = equivalent volume of butene dissolved in the polymer
w = weighting factor for optimal saturation handling
W = parameter defined in Eq. 20
Y = moles of active sites in the reactor
$\underline{Y_{sp}}$ = setpoint trajectory
Y_1 = output variable 1, $\ln(MI_i)$
Y_2 = output variable 2, ρ_i
z^{-1} = backward shift operator

Literature Cited

ASTM, "1990 Annual Book of ASTM Standards," ASTM, Philadelphia, *Volume 8.01 Plastics (1)*, ASTMD 1238 and ASTMD 1505 (1990).

Bequette, B. W., "Nonlinear Control of Chemical Processes: A Review," *Ind. Eng. Chem. Res.*, **30**(7), 1391 (1991).

Burdett, I. D., "The Union Carbide UNIPOL Process: Polymerization of Olefins in a Gas-Phase Fluidized Bed," AIChE Meeting, Washington, DC (Nov. 27-Dec. 2, 1988).

Choi, K. Y., and W. H. Ray, "Recent Developments in Transition Metal Catalyzed Olefin Polymerization—A Survey," *JMS-Rev. Macromol. Chem. Phys.*, **C30**(1), 1 (1985).

Downs, J. J., and J. E. Doss, "A View from North American Industry," *Chemical Process Control—CPC IV*, Y. Arkun and W. H. Ray, eds., *Proc. of Int. Conf. on Chemical Process Control*, Padre Island, TX, CACHE and AIChE, p. 53 (1991).

Freund, E., "Fast Nonlinear Control with Arbitrary Pole-Placement for Industrial Robots and Manipulators," *Int. J. of Robotics Res.*, **1**(1), 65 (1982).

Gagnon, L., and J. F. MacGregor, "State Estimation for Continuous Emulsion Polymerization," *Can. J. of Chem. Eng.*, **69**, 648 (1991).

Garcia, C. E., and M. Morari, "Internal Model Control: 2. Design Procedure for Multivariable Systems," *Ind. Eng. Chem. Process Des. Dev.*, **24**, 472 (1985).

John, P. W. M., *Statistical Methods in Engineering and Quality Assurance*, Wiley, Toronto (1990).

Kozub, D. J., and J. F. MacGregor, "Feedback Control of Polymer Quality in Semi-Batch Copolymerization Reactors," *Chem. Eng. Sci.*, **47**(4), 929 (1992a).

Kozub, D. J., and J. F. MacGregor, "State Estimation for Semi-Batch Polymerization Reactors," *Chem. Eng. Sci.*, **47**(5), 1047 (1992b).

Kozub, D. J., J. F. MacGregor, and T. J. Harris, "Optimal IMC Inverses: Design and Robustness Considerations," *Chem. Eng. Sci.*, **44**(10), 2121 (1989).

Kravaris, C., and C. B. Chung, "Nonlinear State Feedback Synthesis by Global Input/Output Linearization," *AIChE J.*, **33**, 592 (1987).

Krishnan, S., G. W. Barton, and J. D. Perkins, "Robust Parameter Estimation in On-Line Optimization—Part I. Methodology and Simulated Case Study," *Comp. Chem. Eng.*, **16**(6), 545 (1992).

Lee, P. L., and G. R. Sullivan, "Generic Model Control," *Comp. Chem. Eng.*, **12**(6), 573 (1988).

MacGregor, J. F., A. Penlidis, and A. E. Hamielec, "Control of Polymerization Reactors—A Review," *Polym. Proc. Eng.*, **2**, 179 (1984).

McAuley, K. B., "Modelling, Estimation and Control of Product Properties in a Gas Phase Polyethylene Reactor," PhD Thesis, McMaster University, Hamilton, Ontario, Canada (1992).

McAuley, K. B., J. F. MacGregor, and A. E. Hamielec, "A Kinetic Model for Industrial Gas-Phase Ethylene Copolymerization," *AIChE J.*, **36**(6), 837 (1990).

McAuley, K. B., and J. F. MacGregor, "On-Line Inference of Polymer Properties in an Industrial Polyethylene Reactor," *AIChE J.*, **37**(6), 825 (1991).

McAuley, K. B., and J. F. MacGregor, "Optimal Grade Transitions in a Gas-Phase Polyethylene Reactor," *AIChE J.*, **38**, 1564 (1992).

McLellan, P. J., T. J. Harris, and D. W. Bacon, "Error Trajectory Descriptions of Nonlinear Controller Designs," *Chem. Eng. Sci.*, **45**(10), 3017 (1990).

Segall, N. L., J. F. MacGregor, and J. D. Wright, "One-Step Optimal Saturation Correction," *Automat.*, **27**(1), 135 (1991).

Spong, M. W., J. S. Thorpe, and J. M. Kleinwaks, "The Control of Robot Manipulators with Bounded Input," *IEEE Trans. on Automatic Control*, **AC-31**(6), 483 (1986).

Tait, P. J., "Monoalkene Polymerization: Ziegler-Natta and Transition Metal Catalysts," *Comprehensive Polymer Science*, G. Allen and J. C. Bevington, eds., Pergamon Press, Chap. 1, p. 1 (1989).

Appendix: Derivation of the Linear IMC Controller

The first-order decoupled error trajectory in Eq. 8 corresponds to the following discrete time equivalent:

$$\underline{e}(t+h) = \underline{M}\,\underline{e}(t) \tag{A1}$$

where h, the discretization interval for the linear controller, has been chosen to correspond to the sampling time of the on-line GC. The elements of diagonal matrix $\underline{M}$ correspond to $\exp(-h/\tau_i)$ where $\tau_i = -1/\kappa_i$ is the desired first-order closed-loop time constant of the ith error response.

If time-invariant linear transfer function models are sufficient to predict the instantaneous product properties in the gas-phase polyethylene reactor, then one can write:

$$\underline{Y}(t) = \underline{G_p}\,\underline{u}(t) + \underline{D}\,\underline{v}(t) + \underline{d}(t) \tag{A2}$$

where $\underline{G_p}$ is a 2×2 discrete transfer function matrix which relates the manipulated variables u_1 and u_2 to the outputs Y_1 and Y_2. $\underline{D}$ is a 2×4 transfer function matrix which describes how the feedforward variables, $\underline{v}$, affect the output. The elements of $\underline{v}$ are the reactor temperature setpoint, the bleed valve position, the catalyst feed rate, and the bed level setpoint. $\underline{d}(t)$ is a vector of unmeasured disturbances (such as the effects of impurity and catalyst variations on the outputs) which are not accounted for in the transfer function models.

The error trajectory specification in Eq. A1 can be rewritten as:

$$\underline{Y}_{sp}(t+h) - \underline{Y}(t+h) = \underline{M}\{\underline{Y}_{sp}(t) - \underline{Y}(t)\} \tag{A3}$$

Substituting for $\underline{Y}(t+h)$ and $\underline{Y}(t)$ from Eq. A2 gives:

$$\underline{Y}_{sp}(t+h) - \underline{G_p}(t+h) - \underline{D}\,\underline{v}(t+h) - \underline{d}(t+h) = \underline{M}\{\underline{Y}_{sp}(t) - \underline{G_p}\,\underline{u}(t) - \underline{D}\,\underline{v}(t) - \underline{d}(t)\} \tag{A4}$$

Assuming that the best forecast for future values of the disturbance is its current value, that is $\underline{d}(t)$ is a random walk or a series of steps, Eq. A4 becomes:

$$\underline{M}\,\underline{G_p}\,\underline{u}(t) - \underline{G_p}\,\underline{u}(t+h) = \underline{M}\,\underline{Y}_{sp}(t) - \underline{Y}_{sp}(t+h) - \underline{M}\,\underline{D}\,\underline{v}(t) + \underline{D}\,\underline{v}(t+h) - (\underline{M}-\underline{I})\,\underline{d}(t+h) \tag{A5}$$

In Eq. A2, all of the terms in the $\underline{G_p}$ and $\underline{D}$ matrices contain two sampling intervals of delay, one for the zero-order hold, and one for the gas composition measurement deadtime. Each of these matrices can be factored as follows:

$$\underline{G_p} = z^{-2}\underline{\tilde{G}_p} \tag{A6}$$

$$\underline{D} = z^{-2}\underline{\tilde{D}} \tag{A7}$$

where the undelayed portion of the transfer function model, $\underline{\tilde{G}_p}$, is assumed invertible. If G_p is not invertible due to poles outside the unit circle, then approximate model inverses can be obtained in several ways (Garcia and Morari, 1985; Kozub et al., 1989). Substituting $z^{-1}\underline{u}(t+h)$ for $\underline{u}(t)$ in Eq. A5 and right multiplying by $\underline{\tilde{G}_p}^{-1}(\underline{M}z^{-1}-I)^{-1}$ gives:

$$z^{-2}\underline{u}(t+h) = \underline{\tilde{G}_p}^{-1}z^{-1}\underline{Y}_{sp}(t+2h) - \underline{\tilde{G}_p}^{-1}\underline{\tilde{D}}z^{-2}\underline{v}(t+h) - \underline{\tilde{G}_p}^{-1}\underline{F}z^{-1}\underline{d}(t+h) \tag{A8}$$

where

$$\underline{F} = (\underline{I} - \underline{M}z^{-1})^{-1}(\underline{I} - \underline{M}) \quad \text{(A9)}$$

is a first-order filter involving only the specified error trajectory (or desired closed-loop time constant) parameters. Dividing both sides of Eq. A8 by z^{-1} and assuming that $\underline{d}(t+h) = \underline{d}(t)$ leads to the following expression for the control law:

$$\underline{u}(t) = \underline{\tilde{G}}_p^{-1}\underline{Y}_{sp}(t+2h) - \underline{\tilde{G}}_p^{-1}\underline{\tilde{D}}\underline{v}(t) - \underline{\tilde{G}}_p^{-1}\underline{F}\underline{d}(t) \quad \text{(A10)}$$

This linear controller can be implemented in the IMC form shown in Figure 3 wherein $\underline{G}^*$ and $\underline{D}^*$ represent the true process. This is a standard IMC feedback control structure with added feedforward action.

Manuscript received June 25, 1992, and revision received Oct. 20, 1992.